REPRODUCTION
RESEARCH

Initiation of follicular atresia: gene networks during early atresia in pig ovaries

Jinbi Zhang, Yang Liu, Wang Yao, Qifa Li, Honglin Liu and Zengxiang Pan

College of Animal Science and Technology, Nanjing Agricultural University, Nanjing, China

Correspondence should be addressed to H L Liu or Z X Pan; Email: liuhonglin@njau.edu.cn or owwa@njau.edu.cn

Abstract

In mammals, more than 99% of ovarian follicles undergo a degenerative process known as atresia. The molecular events involved in atresia initiation remain incompletely understood. The objective of this study was to analyze differential gene expression profiles of medium antral ovarian follicles during early atresia in pig. The transcriptome evaluation was performed on cDNA microarrays using healthy and early atretic follicle samples and was validated by quantitative PCR. Annotation analysis applying current database (*Sus scrofa* 11.1) revealed 450 significantly differential expressed genes between healthy and early atretic follicles. Among them, 142 were significantly upregulated in early atretic with respect to healthy group and 308 were downregulated. Similar expression trends were observed between microarray data and quantitative RT-PCR confirmation, which indicated the reliability of the microarray analysis. Further analysis of the differential expressed genes revealed the most significantly affected biological functions during early atresia including blood vessel development, regulation of DNA-templated transcription in response to stress and negative regulation of cell adhesion. The pathway and interaction analysis suggested that atresia initiation associates with (1) a crosstalk of cell apoptosis, autophagy and ferroptosis rather than change of typical apoptosis markers, (2) dramatic shift of steroidogenic enzymes, (3) deficient glutathione metabolism and (4) vascular degeneration. The novel gene candidates and pathways identified in the current study will lead to a comprehensive view of the molecular regulation of ovarian follicular atresia and a new understanding of atresia initiation.

Reproduction (2018) **156** 23–33

Introduction

In mammalian ovaries, more than 90% of follicles undergo a degenerative process known as atresia (Kerr *et al.* 2013). Pig primordial follicle reserve is formed in the fetal ovary and approximately 5 million primordial follicles are available at puberty (Manabe *et al.* 2004). Under stimulus during each estrous cycle, a number of primordial follicles start to grow and may either continue to reach the pre-ovulatory stage or become atretic at any time during development (Monniaux *et al.* 2014). It has been observed that, during the antral stage of development, the majority of follicles became atretic when they passed the size of 1 mm in diameter. Atresia rate of antral follicles around 3–5 mm in size was extremely increased (Marchal *et al.* 2002). Studies in different developmental stage of antral growing follicles have indicated that follicular atresia was caused by apoptosis of granulosa cells (GC), which were regulated by a delicate balance of pro-survival factor withdrawal and pro-apoptotic factors (Manabe *et al.* 2004, Hatzirodos *et al.* 2014, Liu *et al.* 2014). Earlier transcriptome profiling studies of atretic follicles suggested a diverse recruitment pattern of genes in different developmental stages (Hatzirodos *et al.* 2014, Terenina *et al.* 2016). However, many gaps are still left to be filled during atresia process. In the present paper, we propose a high-throughput microarray study with the purpose of gaining a better understanding of the molecular factors and pathway networks involved in early follicular atresia of medium antral follicles, thereby leading to a comprehensive view of atresia process and a new understanding of atresia initiation.

Materials and methods

Animal and follicles collection

Ovaries were obtained from mature Duroc × Landrace × Yorkshire sows (weight >120 kg; $n = 26$) at a local slaughterhouse and were washed in PBS (pH 7.3). Tissue samples were transported to the laboratory within 1 h in an insulated container with PBS at 4°C. Individual antral follicles, approximately 3–5 mm in diameter, were dissected from the ovaries using small scissors and fine forceps under a surgical dissecting microscope (SZ51; Olympus). It should be noted that follicular dissection is increasingly difficult, and the RNA quality is lower with more advanced atresia. In total, 239 antral follicles were obtained.

Follicles classification

Combined with previous studies, we had performed a comparative study of methods to determine the follicular atresia

ISSN 1470–1626 (paper) 1741–7899 (online)
https://doi.org/10.1530/REP-18-0058
Online version via www.reproduction-online.org

extent and developed consistent criteria for classifying each follicle into healthy (H), early atresia (EA) or progressive atresia (PA) groups in pigs (Zhang *et al.* 2013). Briefly, follicles were firstly classified morphologically (Bjersing 1967, Cheng *et al.* 2008). H follicles are round with a sharp and continuous granulosa cell membrane, fixed and visible cumulus-oocyte complex (COC) (Bortul *et al.* 2003), fine capillary vessels and clear follicular fluid. EA follicles may have visible COC, but show gaps in membrane granulosa cells, less capillary vessels and turbid follicular fluid. PA follicles do not have visible COC or have COC in follicular fluid with dark floccules (Hay *et al.* 1976, Carson *et al.* 1979) (Table 1). Then, we separated follicular components for confirming classification of the follicles with two other characteristics including the ratio of progesterone and 17β-estradiol level (P4/E2) and the antral GC density. Follicles were opened using fine watchmaker forceps, follicular fluid (including antral GCs) and the follicle wall (including theca interna and granulosa layer) from each follicle were separated by centrifugation (6000 ***g***, 5 s) using a homemade microsieve, which pore size was about 1.5 mm in diameter, fixed inside an 1.5 mL Eppendorf (EP) tube. After re-suspending antral GCs immediately in follicular fluid, 10 µL aliquots of follicular fluid from were diluted in 40 µL PBS in another tube for granulosa cells (ones that comes out spontaneously with follicular fluid) density analysis. The remaining follicular fluid was centrifuged again (6000 ***g***, 20 s). Five microliters aliquots of supernatant were diluted and kept at −80°C for subsequent E2 and P4 assay. The granulosa wall, COC and GCs remaining in the precipitate were stored at −80°C for later RNA extraction. Meanwhile, E2 and P4 levels were retrospectively measured using chemiluminescent kits (Shenzhen Labkit Bioscience Co., Ltd., Shenzhen, China) to confirm the follicle classification. According to previous findings (Sugimoto *et al.* 2001, Maeda *et al.* 2007) and our study (Zhang *et al.* 2013), follicles with a P4/E2 ratio of <5 were classified as H, 5 to 20 as EA and >20 as PA. In addition, number of the antral granulosa cells in follicular fluid was counted using a hemocytometer, and the density was calculated based on the counting results. Densities of <250 cells/µL were classified as H, 250–1000 cells/µL were classified as EA and >1000 cells/µL were classified as PA. Based on a uniform determination among the above three criteria (morphological feature, P4/E2 ratio and the density of granulosa cells), we selected H, EA and PA follicles for further study.

Total RNA isolation and purification for microarray analysis and PCR

After uniform determination among the criteria described earlier, we picked nine follicles for microarray including H ($n=3$), EA ($n=3$) and PA follicles ($n=3$). Then, three follicle samples of each group were pooled together as one mixed sample. Additionally, 30 follicles including H ($n=10$), EA ($n=10$) and PA follicles ($n=10$) were picked for PCR verification. Total RNA of the follicle samples was extracted with TRIzol reagent (Invitrogen) and further purified with an RNeasy mini kit (Qiagen) according to the manufacturers' instructions. Total RNA was quantified by spectrophotometer. The integrity test of purified total RNA was assessed by agarose gel (containing 1.2% formaldehyde) electrophoresis analysis. The subsequent hybridization of microarray slides was performed by the CapitalBio Corporation (Beijing, China).

Microarray hybridization and data analysis

After RNA quality test for microarray, the PA follicles sample was excluded from microarray hybridization because of insufficient RNA quality, thus two microarrays were used in this study, corresponding to the RNAs from H and EA follicles. According to the Affymetrix Expression Analysis Technical Manual (CapitalBio Corporation), each RNA sample separately hybridized with the GeneChip Porcine Genome Array (purchased in 2012, Affymetrix), which contained 23,937 probes (23,256 transcripts) representing 20,201 *Sus scrofa* genes. Array scanning and data extraction were carried out following the standard protocol. Quantitative analysis of microarray hybridization was performed using the GeneChip Operating System (GCOS 1.4, Affymetrix). Data normalization and filtering analysis were carried out with DNA-Chip Analyzer (dChip). The signal log ratio (SLR) was used to estimate the changes in transcript level when two arrays were compared (H vs EA). The data were log base 2 transformed. The log base 2 scale is advantageous because each unit then will be equals a two-fold difference. The genes with SLR ≥1 or ≤−1 (two-fold expression change) between H and EA were filtered using Student's *t*-test for significance at a threshold of $P<0.05$, reported as the 'upregulated' or 'downregulated' differential expression. The differentially expressed genes (DEGs) were then annotated by the latest version (Revision 6) of the Affymetrix porcine annotation (Tsai *et al.* 2006) and combining with the current annotation data of pig (*Sus scrofa* 11.1) in NCBI.

Expression pattern, function enrichment and pathway analysis of DEGs

To recognize the main biological functions that DEGs exercise, we mapped all DEGs to terms in KEGG database and gene ontology (GO) database and looked for significantly enriched terms comparing to the porcine genome background. DEGs were functionally grouped into GO networks using the Cytoscape v3.6.0 software (http://cytoscape.org/index.php)

Table 1 The morphological criteria for follicle classification.

Classification	Transparency	Color	COC	GC layers
Health (H)	Clear	Rosy	Visible	Continuous
Early atresia (EA)	Slightly turbid	Dark orange	Hard to identify	Crenation or partly fell into the antrum
Progressively atresia (PA)	Milky	Gray	Fell into the antrum	Severely fell off and formed deposits

COC, cumulus-oocyte complex.

with the ClueGO plug-in v2.5 (http://www.ici.upmc.fr/cluego/) (Bindea *et al.* 2009). ClueGO established a significant gene-term matrix and biological functional groups for all DEGs at different GO term levels with a threshold of corrected *P* value <0.05. Pathway-based analysis helped to further understand the biological functions of DEGs, which identified significantly enriched metabolic pathways or signal transduction pathways in DEGs comparing with the whole genome background. The statistical significance of the terms analyzed was calculated with two-sided enrichment/depletion hypergeometric test and Bonferroni *P* value correction, taking corrected *P* value <0.05 as a threshold.

Analysis of RNA changes by relative qRT-PCR

To confirm the transcriptional differences observed in the microarray analysis, fluorescent quantitative real-time PCR was carried out on ten selected porcine genes: vascular endothelial growth factor A (*VEGFA*), steroidogenic acute regulatory protein (*STAR*), cytochrome P450 19A1 (*CYP19A1*), radical S-adenosyl methionine domain containing 2 (*RSAD2*), activated leukocyte cell adhesion molecule (*ALCAM*), cytochrome P450, family 11, subfamily A, polypeptide 1 (*CYP11A1*), Fas Ligand (*FASLG*), Tumor Protein P53 (*TP53*), Caspase 3 (*CASP3*) and BCL2 antagonist/killer 1 (*BAK1*) respectively. First-strand cDNA was synthesized using the M-MLV Reverse Transcriptase kit (Promega), according to the manufacturer's protocol. The ten selected genes were detected by real-time PCR using the SYBR Premix Ex Taq (TaKaRa Bio) according to the manufacturer's instructions. Primers were designed based on the porcine mRNA sequences from the GenBank database for all these genes, using the primer Premier 5 software (Premier Biosoft Int., Palo Alto, CA, USA). All primers were synthesized by Invitrogen. Porcine glyceraldeyhyde-3-phosphate dehydrogenase (GAPDH) gene was used as an internal control. The expression level of each target gene was analyzed according to previously described methods (Livak & Schmittgen 2001, Lu *et al.* 2010). The PCR amplification products were analyzed by melting curve analysis and 2% agarose gel electrophoresis, and the results were analyzed using the LightCycler software (ver. 3.5; Roche Diagnostics). Standard curve methods were used to calculate the relative gene expression ratio of a target gene. For each gene, controls for each primer set containing no cDNA were included on each plate, and the reaction was repeated three times for every sample on each plate. The amplification profiles of each gene are shown in Table 2.

Statistical analysis

For gene expression analysis, data were described as mean ± S.E.M. and statistically analyzed using SPSS 20.0 for windows statistical package (SPSS Inc.). Differences with $P<0.05$ were considered statistically significant. For both H and EA follicle groups, the relative mRNA expression levels of the investigated transcripts between were analyzed by the independent-samples *t*-test process.

Results

Microarray hybridization profiles and statistical analysis of DEGs

According to the hybridization signal on the two arrays, the transcriptional profiles of ovarian follicles were determined. A total of 12,601 probe sets (52.64% of

Table 2 Primer and PCR reaction conditions for real-time PCR.

Gene	Accession No.	Primer sequence	Size	Annealing temperature (°C)
VEGFA	NM_214084	F: CCTTGCTGCTCTACCTCC R: CTCCAGACCTTCGTCGTT	239	60
STAR	NM_213755	F: ACTTTGTGAGTGTCGGCTGTA R: CGCTTTCGCAGGTGATT	274	58.6
CYP19A1	NM_214431	F: GCTGCTCATTGGCTTAC R: TCCACCTATCCAGACCC	187	60.8
RSAD2	KC109004.1	F: GGAAAGGGTATGATGAAGA R: GAATTTGTTCCTTGACCC	219	60
ALCAM	XM_013982482.1	F: CCAGAACACGATGAGGCAGACG R: CAGAGCAGCAAGGAGGAGACC	108	60
CYP11A1	DN837451.1	F: AGACACTGAGACTCCACCCCA R: GACGGCCACTTGTACCAATGT	120	65.0
FASLG	AY033634	F: TGGAATTGCCTTGGTCTC R: CATCTTTCCCTCCATCAG	190	56
TP53	AF098067	F: TGACTGTACCACCATCCACTAC R: AAACACGCACCTCAAAGC	143	56.2
CASP3	NM_214131	F: TGGATGCTGCAAATCTCA R: TCCCACTGTCCGTCTCAA	327	58
BAK1	XM_001928147	F: CGGGACACGGAGGAGGTTT R: CCAGAAGAGCCACCACTCG	313	58.5
GAPDH	AF017079	F: GATGGTGAAGGTCGGAGTG R: CGAAGTTGTCATGGATGACC	500	58.0

ALCAM, activated leukocyte cell adhesion molecule; BAK1, BCL2 antagonist killer 1; CASP3, apoptosis-related cysteine peptidase; CYP11A1, cytochrome P450 11A1; CYP19A1, cytochrome P450 19A1; FASLG, FAS ligand; GAPDH, glyceraldehyde 3-phosphate dehydrogenase; RSAD2, radical S-adenosyl methionine domain containing 2; STAR, steroidogenic acute regulatory protein; TP53, tumor suppressor p53; VEGFA, vascular endothelial growth factor A.

all probe sets) were identified to be expressed in the H follicles, 13,541 (56.57%) in the EA follicles and 11,858 (49.54%) in both. At the cutoff criteria of more than two-fold change (SLR ≥1) and $P<0.05$ when comparing between two groups, a total of 556 transcripts (2.39% of total transcripts on the array) were differentially expressed between H and EA follicles, 164 (0.71%) of which were upregulated in EA with respect to H group, while 392 (1.69%) were downregulated. Further functional annotation analysis identified 450 functional genes in current annotation database (*Sus scrofa* 11.1), representing 142 and 308 significantly upregulated and downregulated genes respectively (Table 3).

Validation of microarray data by quantitative RT-qPCR

We performed SYBR green-based quantitative RT-PCR (qRT-PCR) to validate the expression level of six DEGs identified by microarrays with 30 follicles (10 for H, EA and PA respectively). The mRNA levels of PA follicles were detected by PCR although they were not up to standard for microarray detection. We observed a significant correlation between qRT-PCR results and microarray data. All the six genes were of the similar expression trends in both methods, which indicated the reliability of the microarray analysis. Expression in PA group suggested a progressed change during atresia process (Fig. 1). In addition, four typical apoptosis-related genes including *FASLG*, *TP53*, *CASP3* and *BAK1* were also detected by qRT-PCR. Although these genes were not significantly changed in microarray detection which only involved H and EA follicles, a significantly increase was observed when analyzing the expression level of these genes in PA group (Fig. 2).

GO analysis

To further investigate the biological relevance of all the DEGs, the functional categories of DEGs were determined by the GO annotations (http://www.geneontology.org/GO.database.shtml). According to the analysis outcome, 450 DEGs were categorized into 89 significant functional groups, including 45 biological processes, 24 cellular components and 20 molecular functions annotation (Fig. 3). A total of 182 genes were significantly termed as biological process. From the view of % associated genes (enrichment factor), the top five dominant GO

Table 3 Number of DEGs in atretic follicles with respect to healthy follicles.

P value	SLR[a]	Upregulated	Downregulated	Total
$P<0.05$	≥1	122	239	361
	≥2	12	36	48
	≥3	8	33	41
Total		142	308	450

[a]SLR, signal log ratio, which represented the log base 2 transformed fold change of the DEG expression level in EA compare to H follicles.

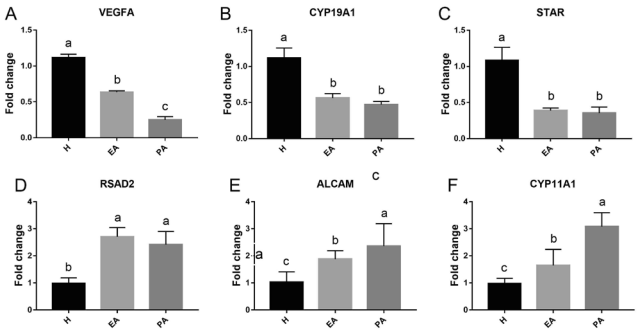

Figure 1 To validate the microarray result, gene expression levels of three downregulated genes including *VEGFA* (A), *CYP19A1* (B), *STAR* (C) and three upregulated genes including *RSAD2* (D), *ALCAM* (E) and *CYP11A1* (F) were detected by qRT-PCR in H, EA and PA groups. Note: The different small letters indicate $P<0.05$. EA, early atresia; H, healthy; PA, progressive atresia; qRT-PCR, quantitative RT-PCR.

terms were labyrinthine layer blood vessel development, regulation of DNA-templated transcription in response to stress, placenta blood vessel development, negative regulation of cell adhesion and regulation of chemotaxis in the biological process groups respectively. We also observed a high percentage of genes in the biological process group that were closely associated with signal transduction, metabolic process, response to stress or stimulus, blood vessel development or morphogenesis. From the cellular component perspective, 71 genes were significantly termed as this ontology, of which many genes were clustered into extracellular matrix, chromatin and nuclear chromosome part. Additionally, in the molecular function category, the dominant categories were molecular-binding activity, signaling

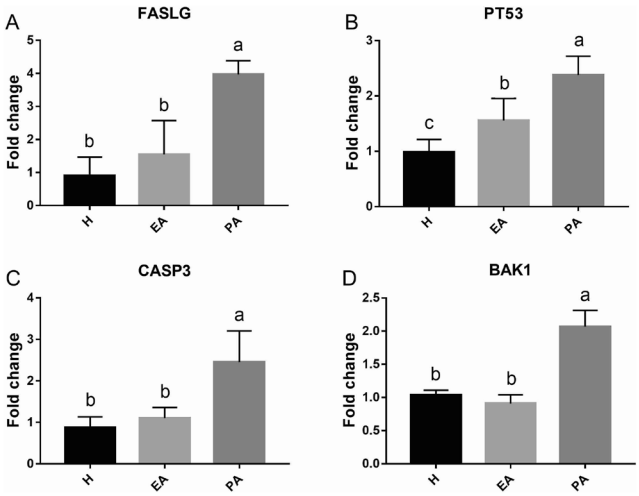

Figure 2 Gene expression levels of four apoptosis-related genes including *FASLG* (A), *TP53* (B), *CASP3* (C) and *BAK1* (D) were detected by qRT-PCR. Significantly increases were observed in PA group with respect to H and EA groups. Note: The different small letters indicate $P<0.05$. EA, early atresia; H, healthy; PA, progressive atresia; qRT-PCR, quantitative RT-PCR.

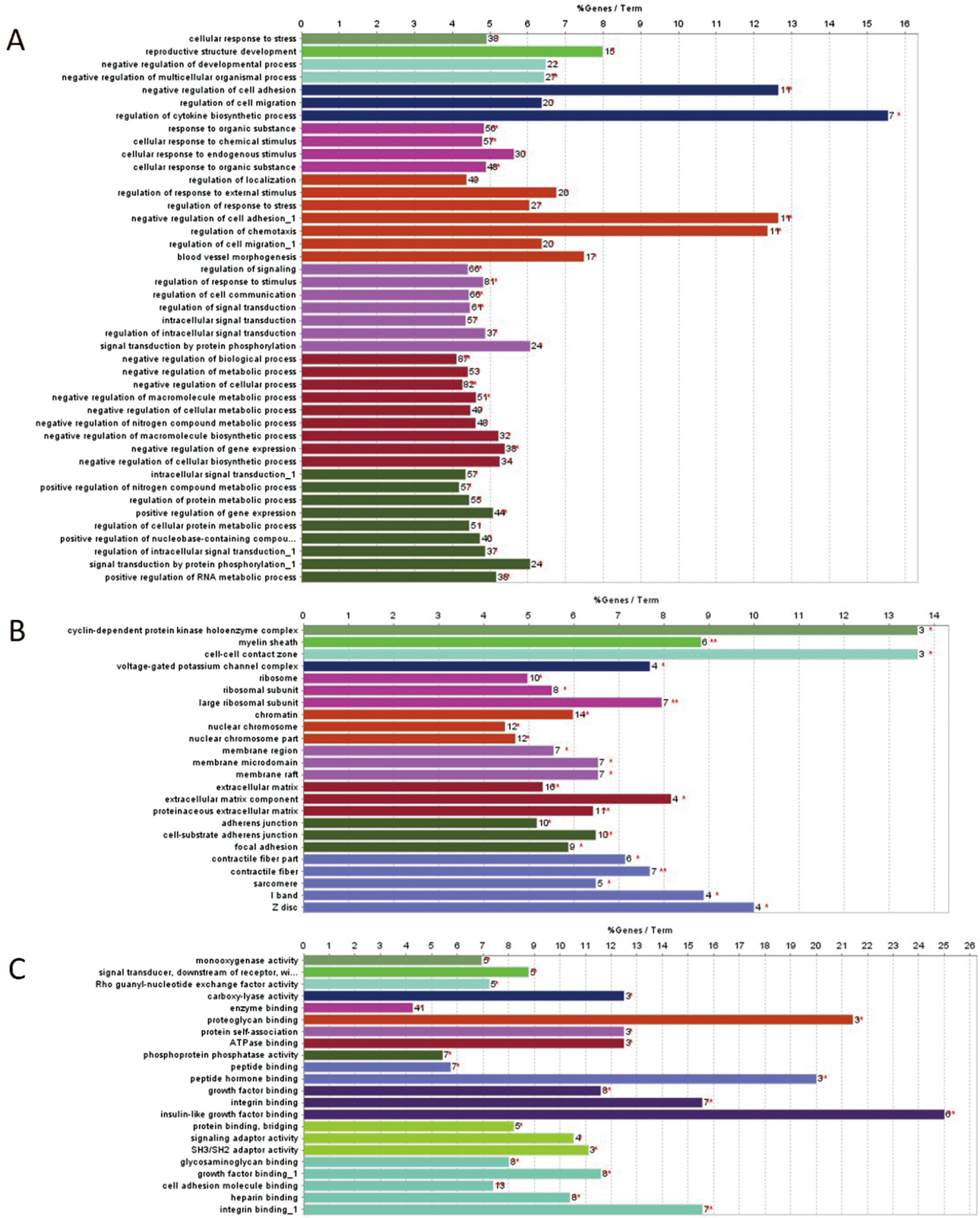

Figure 3 GO analysis was performed using DEGs between H and EA follicles. The 2D bar graph of biological process (A), cellular components (B) and molecular functions (C) categories was generated by ClueGO. The vertical axis shows terms GO categories and the horizontal axis shows the percentage of DEGs out of all genes included in each term. Numbers in the end of each bar represent number of DEGs. Terms with same color represents groups consisting of terms with interrelations. DEG, differentially expressed genes.

adaptor or transducer activity, which consisted of 86 annotated genes.

Pathway analysis of DEGs to characterize the transcriptomic shift during atresia initiation

To further understand the role of these DEGs in physiological functions during ovarian follicular atresia, we mapped them to terms in the KEGG database (http://www.genome.ad.jp/kegg/). KEGG analysis indicated that 41 potential signaling pathways, which involved 129 genes, were related to early follicular atresia. A bubble chart was used to visualize main pathways and number of related DEGs (Fig. 4) and the detailed information of all pathways was listed in Table 4. The key pathways involved in the porcine follicular atresia including ferroptosis, ovarian steroidogenesis, glutathione metabolism, HIF-1 signaling pathway, TGF-beta signaling pathway, FoxO signaling pathway and so forth. Predicted pathways and the corresponding DEGs will be of strong interest for researchers to conduct further investigation and verification analysis in porcine follicular atresia. We also examined potential pathway interactions of the 450 DEGs. The pathway interaction analysis revealed seven associated pathway groups (Fig. 5). In particular, the pathway interaction involved in ovarian steroidogenesis, longevity regulating pathway, autophagy and mitophagy, which included 15 genes (*CYP11A1*, *CYP19A1*, *IGF1R*, *INSR*, *PRKACB*, *STAR*, *ATG5*, *HSPA1B*, *GABARAPL1*, *HIF1A*, *ITPR1*, *MAPK9*, *TP53INP2*, *ATF4*, *TFEB*) was highlighted.

Discussion

Follicle atresia is a complicated process that limits the potential reproduction power of domestic animals. In this study, a comprehensive gene expression profiling by means of microarray analysis was applied to identify groups of genes differently expressed in pig ovary follicles during atresia. Similar microarray approaches have been used previously to characterize healthy antral follicles during growth (Bonnet *et al.* 2008) and small (measuring 1–2 mm) follicles during atresia (Terenina *et al.* 2016). However, the present study is the first gene array analysis investigating health and early atretic medium (measuring 3–5 mm) antral follicles in pigs with 450 DEGs highlighted according to the latest pig genome annotation. When compared with Terenina's work (Terenina *et al.* 2016), we found that overlapping rates of upregulated or downregulated DEG were less than 10%, which suggests that follicles of different development stages (which require different classification methods) may apply very different atretic mechanisms. Based on our findings, the following aspects may be involved in the initiation of follicular atresia.

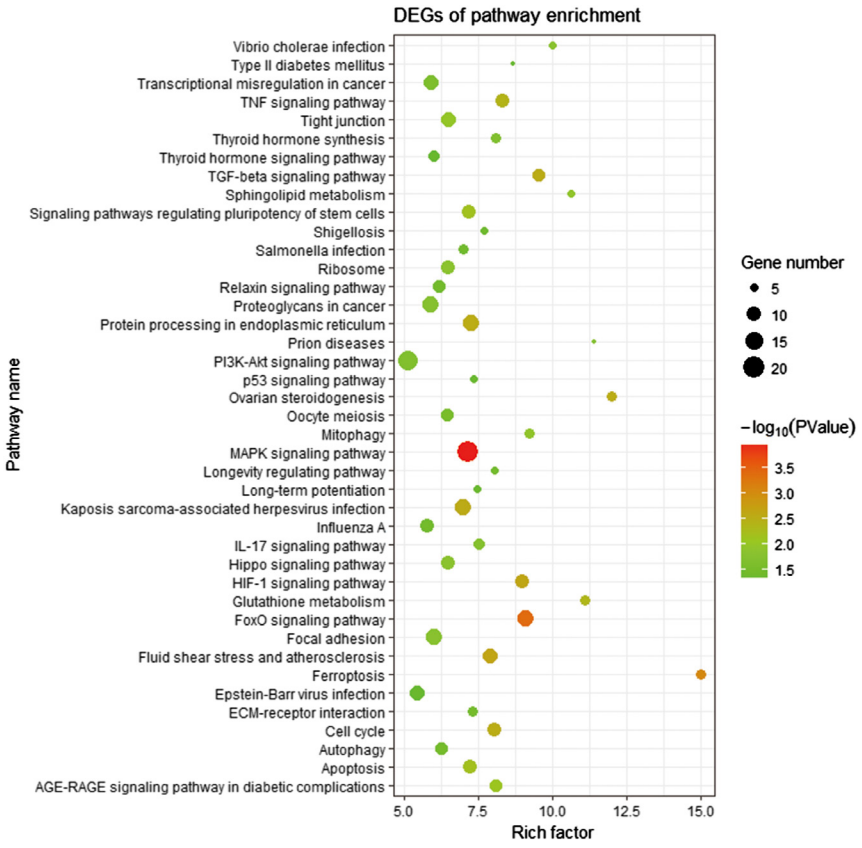

Figure 4 Bubble chart of potential signaling pathways generated by DEGs. Pathway analysis was performed to associate the unique DEGs with pathways using the KEGG database. The size and color of each bubble represent number of DEGs in each pathway and *P* value respectively. DEG, differentially expressed genes.

Table 4 Potential pathways involved in atresia initiation indicated by KEGG analysis.

KEGG ID	Pathway term	Gene No.	% Associated genes	*P* value	Associated genes found
4216	Ferroptosis	6	15.00	9.06E-04	*ACSL1, ATG5, GCLC, PCBP2, SLC7A11, TF*
4913	Ovarian steroidogenesis	6	12.00	2.95E-03	*CYP11A1, CYP19A1, IGF1R, INSR, PRKACB, STAR*
5020	Prion diseases	4	11.43	1.75E-02	*C7, EGR1, LAMC1, PRKACB*
480	Glutathione metabolism	6	11.11	4.36E-03	*GCLC, GPX5, GSTA1, GSTA2, IDH2, MGST2*
600	Sphingolipid metabolism	5	10.64	1.09E-02	*ASAH1, KDSR, SGMS1, SPTLC3, UGCG*
5110	*Vibrio cholerae* infection	5	10.00	1.41E-02	*ACTB, ATP6V1G2, KDELR3, PRKACB, SEC61A1*
4350	TGF-beta signaling pathway	8	9.52	2.78E-03	*ID1, ID2, ID3, ID4, INHBA, INHBB, MYC, THBS1*
4137	Mitophagy	6	9.23	1.07E-02	*ATF4, ATG5, GABARAPL1, HIF1A, MAPK9, TFEB*
4068	FoxO signaling pathway	12	9.09	4.02E-04	*BCL6, CCND2, FBXO32, GABARAPL1, GADD45B, GADD45G, IGF1R, INSR, KLF2, MAPK9, NLK, TNFSF10*
4066	HIF-1 signaling pathway	9	9.00	2.28E-03	*ANGPT2, EDN1, HIF1A, IGF1R, INSR, RPS6, SERPINE1, TF, VEGFA*
4930	Type II diabetes mellitus	4	8.70	4.27E-02	*INSR, MAPK9, SOCS1, SOCS3*
4668	TNF signaling pathway	9	8.33	3.85E-03	*ATF4, CEBPB, CXCL2, EDN1, JUNB, MAP3K5, MAPK9, SOCS3, TNFAIP3*
4918	Thyroid hormone synthesis	6	8.11	1.95E-02	*ATF4, ATP1A1, GPX5, HSP90B1, ITPR1, PRKACB*
4933	AGE-RAGE signaling pathway in diabetic complications	8	8.08	7.57E-03	*COL1A1, COL3A1, EDN1, EGR1, MAPK9, PLCD3, SERPINE1, VEGFA*
4110	Cell cycle	10	8.06	2.99E-03	*ANAPC5, CCNA2, CCND2, CDC27, CDK7, GADD45B, GADD45G, MYC, YWHAE, YWHAZ*
4213	Longevity regulating pathway	5	8.06	3.26E-02	*ATG5, HSPA1B, IGF1R, INSR, PRKACB*
5418	Fluid shear stress and atherosclerosis	11	7.91	2.18E-03	*ACTB, DUSP1, EDN1, GSTA1, GSTA2, HSP90B1, KLF2, MAP3K5, MAPK9, MGST2, VEGFA*
5131	Shigellosis	5	7.69	3.89E-02	*ACTB, ARPC4, ATG5, MAPK9, VCL*
4657	IL-17 signaling pathway	7	7.53	1.75E-02	*ANAPC5, CEBPB, CXCL2, HSP90B1, MAPK9, SRSF1, TNFAIP3*
4720	Long-term potentiation	5	7.46	4.34E-02	*ATF4, ITPR1, PPP3CA, PRKACB, RAP1A*
4115	p53 signaling pathway	5	7.35	4.58E-02	*CCND2, GADD45B, GADD45G, SERPINE1, THBS1*
4512	ECM–receptor interaction	6	7.32	3.05E-02	*AGRN, COL1A1, LAMB1, LAMC1, THBS1, TNR*
4141	Protein processing in endoplasmic reticulum	12	7.27	2.83E-03	*ATF4, CALR, EIF2AK2, HSP90B1, HSPA1B, HSPH1, MAP3K5, MAPK9, PPP1R15A, SEC61A1, TRAM1, UBQLN1*
4210	Apoptosis	10	7.25	6.40E-03	*ACTB, ATF4, CTSC, GADD45B, GADD45G, ITPR1, LMNA, MAP3K5, MAPK9, TNFSF10*
4550	Signaling pathways regulating pluripotency of stem cells	10	7.19	6.73E-03	*FZD5, ID1, ID2, ID3, ID4, IGF1R, INHBA, INHBB, KLF4, MYC*
4010	MAPK signaling pathway	21	7.14	1.05E-04	*ANGPT2, ATF4, DUSP1, DUSP6, EFNA5, FGF10, GADD45B, GADD45G, HSPA1B, IGF1R, INSR, MAP3K5, MAP4K4, MAPK9, MYC, NLK, PPP3CA, PRKACB, RAP1A, TAOK1, VEGFA*
5167	Kaposi's sarcoma-associated herpes virus infection	13	6.99	2.71E-03	*ANGPT2, CXCL2, EIF2AK2, GABARAPL1, HIF1A, ITPR1, MAPK9, MYC, PPP3CA, PREX1, RCAN1, VEGFA, ZFP36*
5132	*Salmonella* infection	6	6.98	3.74E-02	*ACTB, ARPC4, CXCL2, DYNC2H1, MAPK9, MYH10*
3010	Ribosome	10	6.49	1.34E-02	*RPL12, RPL13A, RPL17, RPL23, RPL24, RPL32, RPL6, RPLP1, RPS6, UBA52*
4390	Hippo signaling pathway	10	6.49	1.34E-02	*ACTB, CCND2, CTGF, FZD5, ID1, ID2, MYC, SERPINE1, YWHAE, YWHAZ*
4530	Tight junction	11	6.47	9.92E-03	*ACTB, ACTR3, CGNL1, HSPA4, MAP3K5, MAPK9, MPDZ, MYH10, PRKACB, RAP1A, RDX*
4114	Oocyte meiosis	8	6.45	2.66E-02	*ANAPC5, CDC27, IGF1R, ITPR1, PPP3CA, PRKACB, YWHAE, YWHAZ*
4140	Autophagy	8	6.25	3.13E-02	*ATG5, GABARAPL1, HIF1A, IGF1R, ITPR1, MAPK9, PRKACB, TP53INP2*

(Continued)

Table 4 Continued.

KEGG ID	Pathway term	Gene No.	% Associated genes	*P* value	Associated genes found
4926	Relaxin signaling pathway	8	6.15	3.39E-02	*ATF4, COL1A1, COL3A1, EDN1, EDNRB, MAPK9, PRKACB, VEGFA*
4919	Thyroid hormone signaling pathway	7	6.03	4.99E-02	*ACTB, ATP1A1, HIF1A, MYC, PLCD3, PRKACB, RCAN1*
4510	Focal adhesion	12	6.03	1.50E-02	*ACTB, CCND2, COL1A1, IGF1R, LAMB1, LAMC1, MAPK9, RAP1A, THBS1, TNR, VCL, VEGFA*
5202	Transcriptional misregulation in cancer	11	5.91	2.25E-02	*BCL6, CCND2, CEBPB, DUSP6, GADD45B, GADD45G, ID2, IGF1R, MYC, NFKBIZ, SLC45A3*
5205	Proteoglycans in cancer	12	5.91	1.66E-02	*ACTB, FZD5, HIF1A, HPSE2, IGF1R, ITPR1, MYC, PRKACB, RDX, RPS6, THBS1, VEGFA*
5164	Influenza A	10	5.78	3.37E-02	*ACTB, EIF2AK2, HSPA1B, IL33, MAPK9, MX1, RSAD2, SOCS3, TNFSF10, XPO1*
5169	Epstein-Barr virus infection	11	5.42	5.00E-02	*AKAP8L, CCNA2, EIF2AK2, HSPA1B, MAPK9, MYC, PRKACB, TNFAIP3, XPO1, YWHAE, YWHAZ*

Cell ferroptosis and apoptosis involved in early and late atretic stage respectively

Ferroptosis, which is a recently defined regulated form of cell death, was highlighted in our result. Ferroptosis is characterized by a production of reactive oxygen species (ROS) from accumulated iron and lipid peroxidation (Dixon *et al.* 2012). A decrease of *TF* (transferrin) and increase of iron chaperone *PCBP* (poly (rC) binding protein 2) in EA follicles implied accumulation of iron, which may lead to ferroptosis in earlier atresia process. The role of apoptosis in atresia, on the other hand, has been argued in previous studies. It has been proposed that apoptosis, which involves activation of a group of caspases, was the main biological process involved in follicular atresia (Tilly 1996*a*,*b*). Expression of apoptosis-related genes such as *CASP3* has been reported in antral follicles of porcine, bovine (Feranil *et al.* 2005) and ovine (Phillipps *et al.* 2011) during atresia and closely related with GC apoptosis. On the contrary, recent studies suggested that none of classical granulosa apoptosis markers such as *FAS* (Fas cell surface death receptor), *BAX* (BCL2-associated X protein) or caspases was significantly different in their expression during atresia in granulosa cells of small-to-large bovine follicles (Douville & Sirard 2014, Hatzirodos *et al.* 2014). Our study in which follicles were separated into healthy, early and progressed atretic stages provided a reasonable explanation of the paradox. Although no typical apoptosis-related genes mentioned earlier were detected to be differentially expressed between H and EA follicles, following qRT-PCR revealed a significant increase of *TP53*, *BAK1*, *FASLG*, *CASP3* especially between PA and H/EA follicles. It is known that activated TP53 locates on mitochondrial membrane to enhance apoptosis by interacting with members of Bcl-2 family such as BAK1 (Wang *et al.* 2015), while FASLG activates FAS apoptosis pathway (Kim *et al.* 1999) and eventually induces CASP3. Taken together, our results combined with previous literature suggest that atresia process involves multiple cell death mechanisms. Ferroptosis mechanism may be involved earlier in atresia stage through accumulation of iron molecules, classical apoptosis mechanisms, however, may start during late stage during atresia.

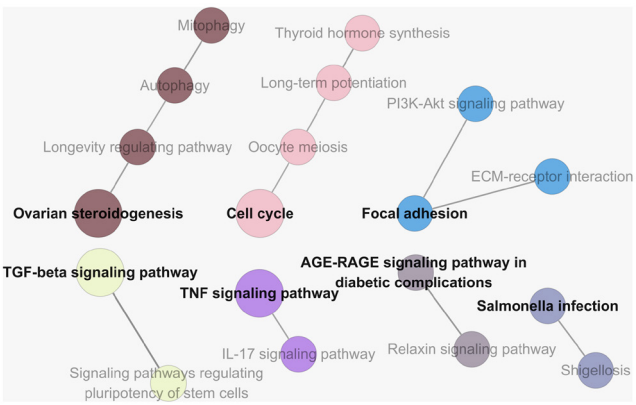

Figure 5 Main pathways and interactions. Pathway analysis was performed using DEGs. Each solid circle represents an individual pathway and the size of each circle indicates number of DEGs included in the pathway. Circles that connected by straight lines represent pathway interactions. DEG, differentially expressed genes.

Autophagy and mitophagy play a role in cellular damage control in EA

Autophagy and mitophagy are cellular processes related to breaking down and reusing of cytoplasm components. Under certain conditions, they may regulate cell death both positively and negatively by cross-talking with apoptosis (Gump *et al.* 2014). The role of autophagy pathway during follicular atresia has started to be valued by researchers recently (Sugiyama *et al.* 2015, Zhou *et al.* 2017). In our microarray results, both *ATG5* (autophagy-related 5) and *GABARAPL1* (GABA type A

receptor-associated protein like 1), which are involved in autophagic vesicle formation, were downregulated during atresia. This trend suggested that autophagy may play a role in apoptosis resistance during EA by preserving energy and safeguarding against accumulation of damaged and aggregated biomolecules. According to our pathway interaction analysis, autophagy and mitophagy pathways are also related to ovarian steroidogenesis. However, further research was required to examine mechanisms of autophagy in granulosa, theca cells and oocytes during follicle development and atresia.

Steroid hormone metabolism involves in the initiation of follicle atresia

Ovarian steroidogenesis pathway was shifted significantly during atresia. Transcriptional levels of *STAR* and *CYP19A1* were significantly greater in healthy follicles, while level of *CYP11A1* and *SULT1E1* (estrogen sulfotransferase) were significantly upregulated during atresia process. It is known that STAR is responsible for cholesterol transportation, which provides substrate for further steroidogenesis. P450arom, on the other hand, is the key enzyme in the synthesis of E2. Greater levels of these two genes are consistent with the fact that sufficient E2 is necessary for follicle maintenance and development (Goldenberg *et al.* 1969, Mcnatty *et al.* 1979). These findings are in agreement with expression pattern of *CYP19A1,3* in small pig follicles (Terenina *et al.* 2016) and the description of *CYP19A1* as an accurate indicator of follicular health in medium bovine follicles (Douville & Sirard 2014). Besides, as a key enzyme in E2 homeostasis (Cole *et al.* 2010), *SULT1E1* upregulation may affect E2 activity in early atretic follicles, which already lack E2 production due to lower level of steroidogenic enzymes, and thus leads to aggravation of atresia. On the other hand, P450scc catalyzes the formation of pregnenolone, which is the substrate for both P4 and E2. Upregulation of *CYP11A1* and downregulation of *CYP19A1* in atretic follicle suggests that abnormal P4 and further androgen production and lack of E2 affect the internal environment of follicles, which may be the major activator in atresia initiation.

Glutathione metabolism and oxidative stress

A greater expression of *GSTA1, A2* (glutathione S-transferase A1, A2), *MGST2* (microsomal glutathione S-transferase 2), *GPX5* (glutathione peroxidase) and *GLUL* (glutamate-ammonia ligase) was observed in H than in EA follicles, which implied the involvement of oxidative stress and glutathione metabolism during atresia process. Under normal physiological conditions, there is a balance maintained between oxidants and antioxidants in cells. However, the excessive production of ROS leads to oxidative stress, which may trigger cell apoptosis or autophagy. *In vitro* studies proved that oxidative stress induces GC apoptosis in mouse and porcine ovaries (Shen *et al.* 2012, Liechuan *et al.* 2016). GSTs function in detoxification process of oxidative stress metabolites and environmental toxins by conjugating with glutathione. GSTA1 and 2 are highly expressed in GC and hormonally regulated by gonadotropins (Rabahi *et al.* 1999). In pig small antral follicles (1–2 mm in diameter), transcription levels of GSTA1, 4 and 5 were also greater in healthy follicles than in atretic ones (Terenina *et al.* 2016). Taken together, greater GSTA1, 2 and microsomal GST expressions may represent a better detoxification capability in healthy follicles, independent of their diameters. In addition, both glutathione peroxidases and glutamine synthetase belong to the ROS scavenging system, which further suppressed free radical damage in healthy follicles.

HIF-1 signaling and vascular regression

HIF-1 signaling pathway is also highlighted in our study. Besides the downregulation of both *HIF1A* (hypoxia inducible factor 1 alpha subunit) and *IGF1R* in early atretic follicles, the shifts of other DEGs including downregulated *VEGFA* and upregulated A*NGPT2* (angiopoietin 2) and *TBXAS1* (thromboxane A synthase 1) suggest that atresia is closely related to angiogenesis process. Angiogenesis plays a role in extensive physiological and pathological processes. In mammal ovary, follicular capillary networks are located in theca interna and make an important contribution to follicular development. HIF1A is mediated by IGF1 and functions as a master regulator of cellular response to hypoxia by activating transcription of downstream genes. Dropping of HIF1 during atresia may directly downregulate the transcription of VEGFA, which regulates angiogenesis by specifically acting upon vascular endothelial cells. Consistent with our results, VEGFA mRNA or protein was detected in the antral follicles from human (Neulen *et al.* 1998), porcine (Shimizu *et al.* 2002), bovine (Greenaway *et al.* 2004), goat (Bruno *et al.* 2009) and buffalo (Babitha *et al.* 2013) and was proved to be involved in the development of vascular network in follicles and inhibition of follicular atresia (Shimizu *et al.* 2007). Angiopoietin 2 disrupts the connections between endothelium and perivascular cells and promotes cell death and vascular regression (Fagiani & Christofori 2013). In concert with VEGFA, angiopoietin 2 promotes neo-vascularization. During EA, however, with the sharp decline of VEGFA, ANGPT2 alone may induce endothelial cell apoptosis with consequent vascular regression. Moreover, endoplasmic reticulum membrane protein *TBXAS1* catalyzes the conversion of prostaglandin H2 (PGH2) to thromboxane A2 (TXA2), which is a potent vasoconstrictor and inducer of platelet aggregation (Minami *et al.* 2015). Based on their functions, we speculate firstly that greater *HIF1A* and *VEGFA* levels in healthy follicles play a role in

growth of follicular vascular networks, and thus provide necessary nutrition supply to maintain healthy follicle development. Secondly, greater *ANGPT2* and *TBXAS1* levels in early atretic follicles may imply a programmed vascular regression mechanism during atresia.

In summary, our study provides a comprehensive profile of DEGs between healthy and early atretic antral follicles in pig. Following bioinformatic analysis suggests (1) a crosstalk of cell apoptosis, autophagy and ferroptosis participates during EA process. However, change of typical apoptosis markers only happens in late atretic stage. (2) Dramatic shift of steroidogenic enzymes and glutathione metabolism affect the environment of follicular fluid during early stage of atresia. (3) Vascular degeneration also plays a role in atresia initiation. In future studies, intensive study of pathways discussed above will offer a deeper understanding of atresia initiation mechanisms. Moreover, particularity study of theca cell, membrana granulosa cell and COC/oocyte respectively will bring a much more comprehensive view of this process.

Declaration of interest

The authors declare that there is no conflict of interest that could be perceived as prejudicing the impartiality of the research reported.

Funding

This work was supported by the National Natural Science Foundation of China (No. 31672421), the Natural Science Foundation of Jiangsu Province (No. BK20160721 and BK20161453), the Fundamental Research Funds for the Central Universities (No. Y0201600160) and the Key Program of the National Natural Science Foundation of China (No. 31630072).

References

Babitha V, Panda RP, Yadav VP, Chouhan VS, Dangi SS, Khan FA, Singh G, Bag S, Taru SG & Silvia WJ 2013 Amount of mRNA and localization of vascular endothelial growth factor and its receptors in the ovarian follicle during estrous cycle of water buffalo (Bubalus bubalis). *Animal Reproduction Science* **48** 810–818. (https://doi.org/10.1016/j.anireprosci.2013.01.004)

Bindea G, Mlecnik B, Hackl H, Charoentong P, Tosolini M, Kirilovsky A, Fridman WH, Pagès F, Trajanoski Z & Galon J 2009 ClueGO: a cytoscape plug-in to decipher functionally grouped gene ontology and pathway annotation networks. *Bioinformatics* **25** 1091–1093. (https://doi.org/10.1093/bioinformatics/btp101)

Bjersing L 1967 On the ultrastructure of follicles and isolated follicular granulosa cells of porcine ovary. *Cell and Tissue Research* **82** 173–186.

Bonnet A, Lê Cao KA, Sancristobal M, Benne F, Robert-Granié C, Law-So G, Fabre S, Besse P, De BE & Quesnel H 2008 In vivo gene expression in granulosa cells during pig terminal follicular development. *Reproduction* **136** 211. (https://doi.org/10.1530/REP-07-0312)

Bortul R, Tazzari PL, Cappellini A, Tabellini G, Billi AM, Bareggi R, Manzoli L, Cocco L & Martelli AM 2003 Constitutively active Akt1 protects HL60 leukemia cells from TRAIL-induced apoptosis through a mechanism involving NF-kappaB activation and cFLIP(L) up-regulation. *Leukemia* **17** 379–389. (https://doi.org/10.1038/sj.leu.2402793)

Bruno JB, Celestino JJ, Lima-Verde IB, Lima LF, Matos MH, Araujo VR, Saraiva MV, Martins FS, Name KP *et al*. 2009 Expression of vascular endothelial growth factor (VEGF) receptor in goat ovaries and improvement of in vitro caprine preantral follicle survival and growth with VEGF. *Reproduction, Fertility and Development* **21** 679–687. (https://doi.org/10.1071/RD08181)

Carson RS, Findlay JK, Burger HG & Trounson AO 1979 Gonadotropin receptors of the ovine ovarian follicle during follicular growth and atresia. *Biology of Reproduction* **21** 75–87. (https://doi.org/10.1095/biolreprod21.1.75)

Cheng Y, Maeda A, Goto Y, Matsuda F, Miyano T, Inoue N, Sakamaki K & Manabe N 2008 Changes in expression and localization of X-linked inhibitor of apoptosis protein (XIAP) in follicular granulosa cells during atresia in porcine ovaries. *Journal of Reproduction and Development* **54** 454–459. (https://doi.org/10.1262/jrd.20088)

Cole GB, Keum G, Liu J, Small GW, Satyamurthy N, Kepe V & Barrio JR 2010 Specific estrogen sulfotransferase (SULT1E1) substrates and molecular imaging probe candidates. *PNAS* **107** 6222–6227. (https://doi.org/10.1073/pnas.0914904107)

Dixon SJ, Lemberg KM, Lamprecht MR, Skouta R, Zaitsev EM, Gleason CE, Patel DN, Bauer AJ, Cantley AM & Yang WS 2012 Ferroptosis: an iron-dependent form of nonapoptotic cell death. *Cell* **149** 1060. (https://doi.org/10.1016/j.cell.2012.03.042)

Douville G & Sirard MA 2014 Changes in granulosa cells gene expression associated with growth, plateau and atretic phases in medium bovine follicles. *Journal of Ovarian Research* **7** 50. (https://doi.org/10.1186/1757-2215-7-50)

Fagiani E & Christofori G 2013 Angiopoietins in angiogenesis. *Cancer Letters* **328** 18–26. (https://doi.org/10.1016/j.canlet.2012.08.018)

Feranil JB, Isobe N & Nakao T 2005 Apoptosis in the antral follicles of swamp buffalo and cattle ovary: TUNEL and caspase-3 histochemistry. *Reproduction in Domestic Animals* **40** 111–116. (https://doi.org/10.1111/j.1439-0531.2005.00563.x)

Goldenberg RL, Vaitukaitis JL & Ross GT 1969 Estrogen and follicle stimulating hormone interactions on follicle growth in rats. *Endocrinology* **90** 1492–1498. (https://doi.org/10.1210/endo-90-6-1492)

Greenaway J, Connor K, Pedersen HG, Coomber BL, LaMarre J & Petrik J 2004 Vascular endothelial growth factor and its receptor, Flk-1/KDR, are cytoprotective in the extravascular compartment of the ovarian follicle. *Endocrinology* **145** 2896–2905. (https://doi.org/10.1210/en.2003-1620)

Gump JM, Staskiewicz L, Morgan MJ, Bamberg A, Riches DW & Thorburn A 2014 Autophagy variation within a cell population determines cell fate through selective degradation of Fap-1. *Nature Cell Biology* **16** 47–54. (https://doi.org/10.1038/ncb2886)

Hatzirodos N, Irvingrodgers HF, Hummitzsch K, Harland ML, Morris SE & Rodgers RJ 2014 Transcriptome profiling of granulosa cells of bovine ovarian follicles during growth from small to large antral sizes. *BMC Genomics* **15** 24. (https://doi.org/10.1186/1471-2164-15-24)

Hay MF, Cran DG & Moor RM 1976 Structural changes occurring during atresia in sheep ovarian follicles. *Cell and Tissue Research* **169** 515–529. (https://doi.org/10.1007/BF00218150)

Kerr JB, Myers M & Anderson RA 2013 The dynamics of the primordial follicle reserve. *Reproduction* **146** R205–R215. (https://doi.org/10.1530/REP-13-0181)

Kim JM, Yoon YD & Tsang BK 1999 Involvement of the Fas/Fas ligand system in p53-mediated granulosa cell apoptosis during follicular development and atresia. *Endocrinology* **140** 2307–2317. (https://doi.org/10.1210/endo.140.5.6726)

Liechuan LI, Shen M, Ning C, Guan Z, Jiang Y, Wangjun WU & Liu H 2016 Induction of granulosa cell autophagy and effects in apoptosis by hydrogen peroxide in porcine ovaries. *Journal of Nanjing Agricultural University* **39** 814–818. (https://doi.org/10.7685/jnau.201601001)

Liu J, Du X, Zhou J, Pan Z, Liu H & Li Q 2014 MicroRNA-26b functions as a proapoptotic factor in porcine follicular granulosa cells by targeting Sma- and Mad-related protein 41. *Biology of Reproduction* **91** 146. (https://doi.org/10.1095/biolreprod.114.122788)

Livak KJ & Schmittgen TD 2001 Analysis of relative gene expression data using real-time quantitative PCR and the 2(-Delta Delta C(T)) Method. *Methods* **25** 402–408. (https://doi.org/10.1006/meth.2001.1262)

Lu FZ, Jiang ZY, Wang XX, Luo YH, Li XF & Liu HL 2010 Role of the insulin-like growth factor system in epiphyseal cartilage on the development of Langshan and Arbor Acres chickens, Gallus domesticus. *Poultry Science* **89** 956. (https://doi.org/10.3382/ps.2008-00556)

Maeda A, Inoue N, Matsudaminehata F, Goto Y, Cheng Y & Manabe N 2007 The role of interleukin-6 in the regulation of granulosa cell apoptosis during follicular atresia in pig ovaries. *Journal of Reproduction and Development* **53** 481–490. (https://doi.org/10.1262/jrd.18149)

Manabe N, Goto Y, Matsudaminehata F, Inoue N, Maeda A, Sakamaki K & Miyano T 2004 Regulation mechanism of selective atresia in porcine follicles: regulation of granulosa cell apoptosis during atresia. *Journal of Reproduction and Development* **50** 493–514. (https://doi.org/10.1262/jrd.50.493)

Marchal R, Vigneron C, Perreau C, Balipapp A & Mermillod P 2002 Effect of follicular size on meiotic and developmental competence of porcine oocytes. *Theriogenology* **57** 1523. (https://doi.org/10.1016/S0093-691X(02)00655-6)

Mcnatty KP, Smith DM, Makris A, Osathanondh R & Ryan KJ 1979 The microenvironment of the human antral follicle: interrelationships among the steroid levels in antral fluid, the population of granulosa cells, and the status of the oocyte in vivo and in vitro. *Journal of Clinical Endocrinology and Metabolism* **49** 851. (https://doi.org/10.1210/jcem-49-6-851)

Minami D, Takigawa N, Kato Y, Kudo K, Isozaki H, Hashida S, Harada D, Ochi N, Fujii M & Kubo T 2015 Downregulation of TBXAS1 in an iron-induced malignant mesothelioma model. *Cancer Science* **106** 1296–1302. (https://doi.org/10.1111/cas.12752)

Monniaux D, Clément F, Dalbiès-Tran R, Estienne A, Fabre S, Mansanet C & Monget P 2014 The ovarian reserve of primordial follicles and the dynamic reserve of antral growing follicles: what is the link? *Biology of Reproduction* **90** 2033–2040. (https://doi.org/10.1095/biolreprod.113.117077)

Neulen J, Raczek S, Pogorzelski M, Grunwald K, Yeo TK, Dvorak HF, Weich HA & Breckwoldt M 1998 Secretion of vascular endothelial growth factor/vascular permeability factor from human luteinized granulosa cells is human chorionic gonadotrophin dependent. *Molecular Human Reproduction* **4** 203–206. (https://doi.org/10.1093/molehr/4.3.203)

Phillipps HR, Kokay IC, Grattan DR & Hurst PR 2011 X-linked inhibitor of apoptosis protein and active caspase-3 expression patterns in antral follicles in the sheep ovary. *Reproduction* **142** 855–867. (https://doi.org/10.1530/REP-11-0177)

Rabahi F, Brûlé S, Sirois J, Beckers JF, Silversides DW & Lussier JG 1999 High expression of bovine alpha glutathione S-transferase (GSTA1, GSTA2) subunits is mainly associated with steroidogenically active cells and regulated by gonadotropins in bovine ovarian follicles. *Endocrinology* **140** 3507–3517. (https://doi.org/10.1210/endo.140.8.6886)

Shen M, Lin F, Zhang J, Tang Y, Chen WK & Liu H 2012 Involvement of the up-regulated FoxO1 expression in follicular granulosa cell apoptosis induced by oxidative stress. *Journal of Biological Chemistry* **287** 25727–25740. (https://doi.org/10.1074/jbc.M112.349902)

Shimizu T, Jiang J-Y, Sasada H & Sato E 2002 Changes of messenger RNA expression of angiogenic factors and related receptors during follicular development in gilts. *Biology of Reproduction* **67** 1846–1852. (https://doi.org/10.1095/biolreprod.102.006734)

Shimizu T, Iijima K, Miyabayashi K, Ogawa Y, Miyazaki H, Sasada H & Sato E 2007 Effect of direct ovarian injection of vascular endothelial growth factor gene fragments on follicular development in immature female rats. *Reproduction* **134** 677–682. (https://doi.org/10.1530/REP-07-0268)

Sugimoto M, Manabe N, Kimura Y, Myoumoto A, Imai Y, Ohno H & Miyamoto H 2001 Ultrastructural changes in granulosa cells in porcine antral follicles undergoing atresia indicate apoptotic cell death. *Journal of Reproduction and Development* **44** 7–14. (https://doi.org/10.1262/jrd.44.7)

Sugiyama M, Kawaharamiki R, Kawana H, Shirasuna K, Kuwayama T & Iwata H 2015 Resveratrol-induced mitochondrial synthesis and autophagy in oocytes derived from early antral follicles of aged cows. *Journal of Reproduction & Development* **61** 251–259. (https://doi.org/10.1262/jrd.2015-001)

Terenina E, Fabre S, Bonnet A, Monniaux D, Robert-Granie C, Sancristobal M, Sarry J, Vignoles F, Gondret F & Monget P 2016 Differentially expressed genes and gene networks involved in pig ovarian follicular atresia. *Physiological Genomics* **49** 67. (https://doi.org/10.1152/physiolgenomics.00069.2016)

Tilly JL 1996*a* Apoptosis and ovarian function. *Reviews of Reproduction* **1** 162–172. (https://doi.org/10.1530/ror.0.0010162)

Tilly JL 1996*b* The molecular basis of ovarian cell death during germ cell attrition, follicular atresia, and luteolysis. *Frontiers in Bioscience* **1** d1. (https://doi.org/10.2741/A111)

Tsai S, Cassady JP, Freking BA, Nonneman DJ, Rohrer GA & Piedrahita JA 2006 Annotation of the Affymetrix porcine genome microarray. *Animal Genetics* **37** 423. (https://doi.org/10.1111/j.1365-2052.2006.01460.x)

Wang J, Guo W, Zhou H, Luo N, Nie C, Zhao X, Yuan Z, Liu X & Wei Y 2015 Mitochondrial p53 phosphorylation induces Bak-mediated and caspase-independent cell death. *Oncotarget* **6** 17192–17205. (https://doi.org/ 10.18632/oncotarget.3780)

Zhang J, Lin F, Pan Z, Xueshan MA, Qifa LI & Liu H 2013 Comparative study of methods to determine the follicular atresia extent in pigs. *Journal of Nanjing Agricultural University* **31** 115-119. (https://doi.org/10.7685/j.issn.1000-2030.2013.01.020)

Zhou J, Yao W, Li C, Wu W, Li Q & Liu H 2017 Administration of follicle-stimulating hormone induces autophagy via upregulation of HIF-1α in mouse granulosa cells. *Cell Death and Disease* **8** e3001. (https://doi.org/10.1038/cddis.2017.371)

Received 1 February 2018
First decision 27 February 2018
Revised manuscript received 1 May 2018
Accepted 8 May 2018